Hindawi
International Journal of Energy Research
Volume 2023, Article ID 2000611, 13 pages
https://doi.org/10.1155/2023/2000611

Research Article

A Communication-Assisted Distance Protection for AC Microgrids considering the Fault-Ride-Through Requirements of Distributed Generators

Deming Wang[1,2] **Fei Li**[1] **and Yingliang Li**[1]

[1]Shaanxi Railway Institute, Weinan 714000, China
[2]School of Electronic Engineering, Xi'an Shiyou University, Xi'an 710065, China

Correspondence should be addressed to Deming Wang; wangdming@foxmail.com

Received 21 September 2023; Revised 14 November 2023; Accepted 1 December 2023; Published 16 December 2023

Academic Editor: Arnab Dutta

The conventional overcurrent protection is ineffective in isolating faults in microgrids due to the low fault current levels contributed by inverter-interfaced distributed generations (IIDGs). To extend the microgrid protection methods, the distance protection is considered as a common alternative to detect faults. However, the fault-ride-through (FRT) requirements and the high impedance fault (HIF) detection challenge the application of the conventional distance protection. To solve the two problems, a new inverse-time distance (ITD) protection for medium-voltage AC microgrids was proposed in this paper. The primary ITD protection was designed to meet the FRT requirements, and the backup protection was coordinated to isolate faults. The fault resistance and distributed generation infeed effect on the measured impedance were mitigated by a communication-assisted method proposed in this paper. Owing to the shorter communication channel time in distribution feeders and lower communication investments without a synchronous clock, the proposed method can be used to improve the ITD protection performance. An 11 kV AC microgrid was simulated with different fault types in the islanded mode and grid-connected mode. Time domain simulation verified the effectiveness of the proposed ITD protection.

1. Introduction

Microgrid containing both distributed generation (DG) and load has attracted interest for their salient features. A microgrid can be regarded as a controlled subsystem that reduces transmission losses, diversifies power suppliers, enhances power quality, and improves system reliability [1, 2]. Despite its advantages, the integrated DGs increase burden on the feeder protection system in microgrids [1, 3].

DG integrated via a voltage source converter (VSC) into a microgrid is the main type in the current practice, and it limits the output current to protect its power electronic device [4–6]. The fault current provided by an inverter-interfaced distributed generation (IIDG) is much lower than the one supplied by the upstream network, and the IIDG fault characteristics are different from a synchronous machine-based generation (SMDG), which brings challenges to the application of the conventional feeder protection system [7, 8]. What is more, a DG-based microgrid can operate either in grid-connected mode or islanded mode, increasing difficulties in applying the conventional feeder protection.

To overcome the problems in microgrid protection system, various strategies have been proposed by researchers. Some researchers considered using adaptive protection schemes to solve the problem in microgrids [9–11]. Oudalov and Fidigatti proposed an adaptive microgrid protection based on using numerical directional overcurrent relays and communication system [10]. Offline network status analysis and online transmitting signal operations were the main parts of the novel scheme. According to Sharaf et al. [11], a dual setting overcurrent protection scheme was presented based on the communication system and the microgrid protection problem was solved by using optimisation functions. The result could be affected by the initial values of the algorithm. It is necessary to calculate short-circuit currents and know all possible configurations of microgrids before using the adaptive protection schemes, which complicates the implementation of these approaches. The differential protection methodologies were also developed in medium-voltage AC microgrids [12–14]. A variable tripping time differential protection scheme (VTDPS) was presented by Aghdam et al. [13], which was based on a multiagent system and tested in a synchronous DG-integrated microgrid. Soleimanisardoo et al. [14] proposed a differential protection scheme to isolate faults in an islanded microgrid. The method detected the current frequency differences depending on the injected off-nominal frequency. Although the differential protection approaches can adapt different fault current levels and isolate faults at a high speed, the communication system infrastructure using a precise synchronous clock is relatively costly and the network configuration can affect the performance of the differential protection.

Other approaches were also investigated, including using fault current limiters (FCLs) or energy storage devices to alter the fault current level [15–17], utilising the methods based on the voltage detection [18–21], and implementing the distance protection methodologies [22–30]. Ibrahim et al. proposed an approach to coordinate the protection relays considering the presence of FCL [17]. The FCL impedance values are difficult to determine considering the mutual influence of DGs, and the investments of the storage devices are too significant to apply these approaches. Using the phase differences between the bus voltage and feeder current, Zhang and Mu developed a fault detection method in microgrids with IIDG connection [21]. The voltage-based schemes are strongly dependent on the network topology and less sensitive in the grid-connected operation.

For the features that change very little in different network topologies, it is reasonable to use the distance protection to detect and clear faults in microgrids. Dewadasa et al. [22] proposed an inverse-time admittance (ITA) protection method, which can be regarded as an improved distance protection. A combined distance protection was developed by Lee et al. [24], utilising distance protection relay and directional relay in single-line fault detection. An adaptive distance protection was proposed for the unbalanced faults by Liang et al. [25], and the high-frequency current was used to improve the distance protection performance in [26]. However, it was verified by Liang et al. [25] that it was inefficient to use the harmonic current injection method in high impedance fault (HIF) detection. Since the measured impedance can be easily affected by the presence of the fault resistance, the proposed protection operating time increased during HIF. The communication channel was used to developed distance protection by Biswas and Centeno [27] and Hooshyar et al. [29] in the active distribution network.

Although the distance protection is more sensitive and adaptive compared to the overcurrent protection, there are two main challenges when using distance protection. Firstly, the operating time should meet the fault-ride-through (FRT) requirements, which means the feeder protection should respond faster than the FRT-required time. Secondly, the measured impedance can easily be affected by the presence of fault impedance and DG infeed, leading to a longer operating time or failure in isolating faults. To solve the two problems, a new inverse-time distance (ITD) protection is proposed in this paper. The new ITD protection can detect faults with a shorter time to meet the FRT requirements, and the backup protection can be coordinated to isolate faults. What is more, a communication-assisted method is proposed to mitigate the fault impedance and DG infeed effect on the measured impedance. The structure of this paper is shown as the following. The FRT requirements are presented in Section 2. Section 3 illustrates the proposed ITD protection as well as the mitigating the fault impedance effect method. In Section 4, a protection scheme involving the proposed ITD protection is presented. Case study using MATLAB Simulink is conducted, and the simulation results are presented in Section 5. The time domain simulation results verify the effectiveness of the proposed method.

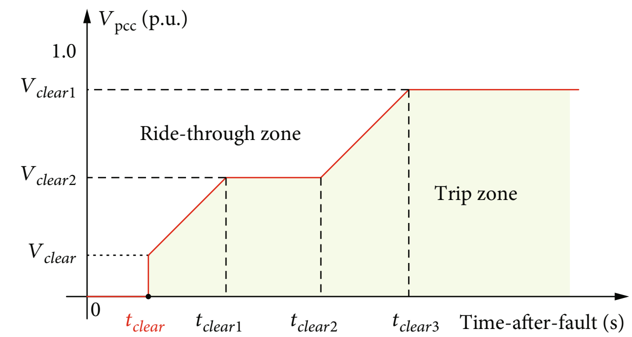

Figure 1: Fault-ride-through requirements.

2. New Inverse-Time Distance Protection

2.1. FRT Requirements. DGs should have the capability to provide reactive power and dynamically support the distribution network voltage during fault conditions, which is often referred to FRT requirements [21, 31]. The general FRT requirements are shown in Figure 1, in which the DG common coupling point (PCC) voltage versus time-after-fault curve is depicted as well as the ride-through zone. DGs should stay connected to the distribution network during a fault for a certain time. The FRT-required time depends on the drop of the PCC voltage (denoted as V_{pcc}), shown as the red line in Figure 1. FRT requirements in different countries possess similar characteristics, and the minimum time t_{clear} is normally selected as 0.15 seconds [1, 4]. To meet the FRT requirements, the operating time of the feeder primary protection should be less than the FRT-required time.

2.2. The Characteristics of ITD Protection. For the operating time that varies along with the fault location, the inverse-time overcurrent relays are predominately implemented in distribution networks. The ITD protection was developed based on the inverse-time characteristics [32, 33], considering the FRT requirements. To illustrate the characteristics of ITD protection, a simplified network is presented in

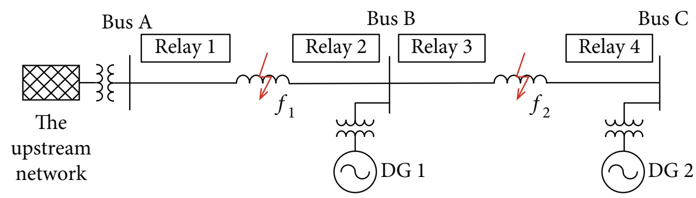

FIGURE 2: A simplified network.

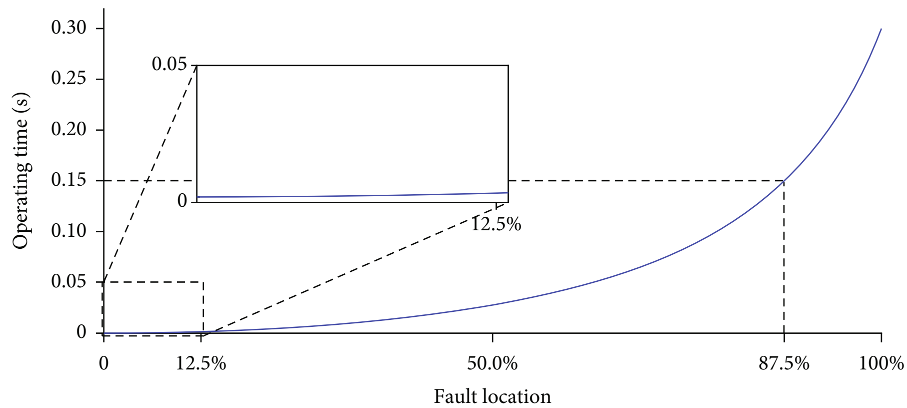

FIGURE 3: The characteristics of ITD primary protection.

Figure 2. DGs are integrated into the network, and relays are implemented at the two terminals of each feeder.

2.2.1. The Primary Protection. The primary protection should detect faults with much less operating time. The characteristics of the primary protection can be described as

$$t_{\mathrm{I}} = \frac{A}{\left[\left|(kZ_{\mathrm{I}})/Z_{\mathrm{m}}\right|^2 - 1\right]}, \tag{1}$$

where t_{I} is the operating time of the primary protection, A is the time dial setting of the primary protection, k is a reliable coefficient which can be selected as 1.2 to cover the whole feeder length, Z_{I} is the impedance of the feeder covered by the primary protection, and Z_{m} is the impedance seen by relays.

The new ITD primary protection is designed to protect the feeder at full length and relays located at the sending side of the series feeders need to be coordinated. The minimum coordination time interval (CTI) between two series relays can be set as 0.3 seconds [9].

$$t_{\mathrm{I}}(Z_{\mathrm{m}} = Z_{\mathrm{I}}) = 0.3. \tag{2}$$

A can be calculated through (1) and (2). It is 0.132 and independent of the feeder length. The proposed ITD primary protection possesses one setting group for different feeder lengths, which is more convenient for application.

The characteristics of the ITD primary protection are presented in Figure 3. It can be seen that the maximum operating time of the ITD primary protection is 0.15 seconds during a fault occurring within 87.5% of the feeder length, which is sufficient for the FRT requirements of DGs.

2.2.2. The Backup Protection. To improve the reliability of the protection system, the ITD protection needs a backup protection scheme, which can be expressed as

$$t_{\mathrm{II}} = \frac{A}{\left[\left|(kZ_{\mathrm{II}})/Z_{\mathrm{m}}\right|^2 - 1\right]} + \Delta t, \tag{3}$$

where t_{II} is the backup protection operating time, Δt is a coordination parameter, and Z_{II} is the impedance of the feeders covered by the backup protection. It is noted that the backup protection can cover the local and adjacent feeder.

The coordination between the primary and backup protection should be considered, and the minimum CTI between the primary and backup protection is set as 0.3 seconds [34].

$$t_{\mathrm{II}}(Z_{\mathrm{m}} = Z_{\mathrm{I}}) = t_{\mathrm{I}}(Z_{\mathrm{m}} = Z_{\mathrm{I}}) + 0.3. \tag{4}$$

Δt can be obtained through (2), (3), and (4) and is given in

$$\Delta t = 0.6 - \frac{A}{\left[\left|(kZ_{\mathrm{II}})/Z_{\mathrm{m}}\right|^2 - 1\right]}. \tag{5}$$

It is to be noticed that relays involving ITD characteristics can detect faults in either side of the relays. The direction can be detected in microgrids, such as utilising the relative phase angle between the prefault and superimposed sequence fault current presented by Muda and Jena [35] or using the postfault current phasor by Hosseini et al. [36]. The main focus is the ITD protection, and the detection of

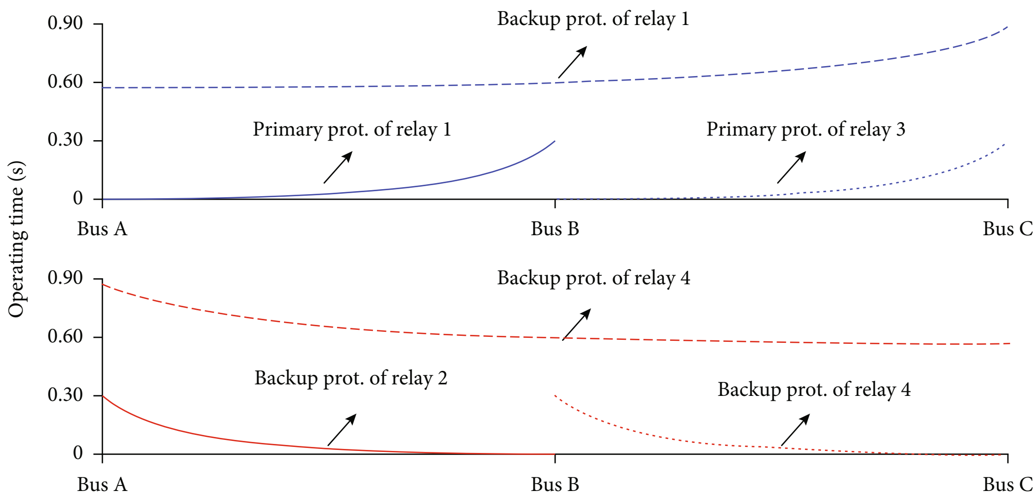

Figure 4: The coordination between ITD primary protection relays and backup protection relays.

the fault direction is not discussed in this paper. It is noted that relays involving ITD protection only respond to forward faults.

To present the characteristics of the proposed ITD protection, the operating time versus fault location curve is depicted in the case when faults are occurring in the sample network (shown in Figure 2). The feeder BC length is the same as the feeder AB length, and the relay ITD characteristics are shown in Figure 4. It can be seen that the operating time of the primary protection can meet the FRT requirements and the backup protection can be coordinated with the primary protection to isolate faults.

2.3. Different Elements of ITD Protection. The ITD protection can detect phase-to-ground faults as well as phase-to-phase faults by utilising different protection elements.

2.3.1. Ground Distance Element. The ground distance element can be used to detect a phase-to-ground fault, which is expressed as

$$Z_{\mathrm{m}} = \frac{\dot{V}_{\text{p-g}}}{\dot{I}_{\text{p-g}} + 3k_0\dot{I}^0}, \tag{6}$$

where $V_{\text{p-g}}$, $I_{\text{p-g}}$, and I^0 are the rms phase fault voltage, the rms phase fault current, and the rms zero-sequence fault current seen by the relays, respectively, and k_0 is the zero-sequence current compensation factor.

$$k_0 = \frac{Z^0 - Z^1}{3Z^1}, \tag{7}$$

where Z^0 and Z^1 are the feeder zero-sequence impedance and the feeder positive-sequence impedance, respectively.

2.3.2. Phase Distance Element. The phase-to-phase faults can be detected by using a phase distance element shown as the following.

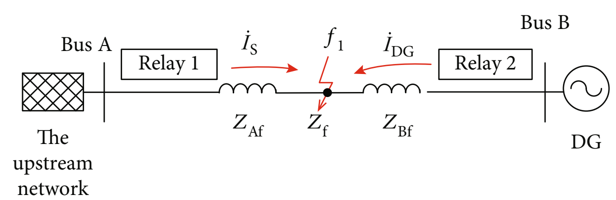

Figure 5: Effect of fault impedance on the measured impedance.

$$Z_{\mathrm{m}} = \frac{\dot{V}_{\text{p-p}}}{\dot{I}_{\text{p-p}}}, \tag{8}$$

where $V_{\text{p-p}}$ and $I_{\text{p-p}}$ are the rms phase-to-phase fault voltage and the rms phase-to-phase fault current seen by the relays, respectively.

2.4. Method to Mitigate the Fault Impedance and DG Infeed Effect. The measured impedance can easily be affected by the presence of fault impedance and DG infeed. To mitigate the effect and improve the ITD performance, a communication-assisted method is proposed.

2.4.1. Mitigating the Fault Impedance Effect. A single phase-to-ground fault with the presence of fault impedance is studied, which is shown in Figure 5. Z_{Af} is the impedance between bus A and f_1, Z_{Bf} is the impedance between bus B and f_1, and Z_{f} is the actual fault impedance existing at the point f_1. I_{S} and I_{DG} are the fault current fed from the upstream network and DG, respectively.

The measured impedance seen by relay 1 and relay 2 can be expressed as

$$Z_{\mathrm{m}(1)} = Z_{\mathrm{Af}} + \left(\frac{\dot{I}^{\mathrm{c}}_{\mathrm{DG}}}{\dot{I}^{\mathrm{c}}_{\mathrm{S}}} + 1\right) Z_{\mathrm{f}}, \tag{9}$$

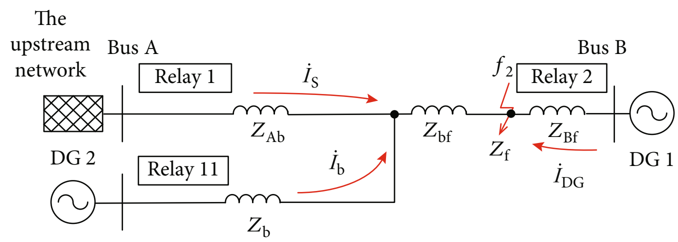

Figure 6: Effect of fault impedance on measured impedance.

$$Z_{m(2)} = Z_{Bf} + \left(\frac{\dot{I}_S^c}{\dot{I}_{DG}^c} + 1\right) Z_f, \tag{10}$$

where

$$\begin{aligned} \dot{I}_{DG}^c &= \dot{I}_{DG} + 3k_0 \dot{I}_{DG}^0, \\ \dot{I}_S^c &= \dot{I}_S + 3k_0 \dot{I}_S^0. \end{aligned} \tag{11}$$

$\dot{I}_S^0$ and $\dot{I}_{DG}^0$ are the zero-sequence fault currents fed from the upstream network and DGs, respectively.

It is to be noticed that the sum of Z_{Af} and Z_{Bf} is the whole impedance of the feeder AB, and the value of Z_f can be calculated through (9) and (10).

$$Z_f^c = \frac{Z_{m(1)} + Z_{m(2)} - Z_{AB}}{\left(\dot{I}_S^c/\dot{I}_{DG}^c\right) + \left(\dot{I}_{DG}^c/\dot{I}_S^c\right) + 2}, \tag{12}$$

where Z_{AB} is the whole impedance of the feeder AB.

The measured impedance without fault impedance interference can be calculated by

$$\begin{aligned} Z_{m(1)}^c &= Z_{m(1)} - \left(\frac{\dot{I}_{DG}^c}{\dot{I}_S^c} + 1\right) Z_f^c, \\ Z_{m(2)}^c &= Z_{m(2)} - \left(\frac{\dot{I}_S^c}{\dot{I}_{DG}^c} + 1\right) Z_f^c, \end{aligned} \tag{13}$$

where $Z_{m(1)}^c$ and $Z_{m(2)}^c$ are the calculated impedance which can substitute the measured impedance ($Z_{m(1)}$ and $Z_{m(2)}$) to improve the performance of ITD protection.

As for the intermittence and randomicity of DGs, the fault impedance can also be calculated by (14) in the case when DG is out of operation.

$$Z_f^c = \frac{\dot{V}_{m(2)}}{\dot{I}_S^c}, \tag{14}$$

where $\dot{V}_{m(2)}$ is the fault voltage seen by relay 2.

2.4.2. Mitigating the Infeed Effect. When there is a DG infeed, the measured impedance seen by the relays can also be affected. Figure 6 shows the DG infeed effect, in which Z_b represents the infeed branch impedance and I_b denotes the infeed current.

The measured impedance seen by relay 1, relay 2, and relay 3 can be expressed as

$$\begin{aligned} Z_{m(1)} &= Z_{Ab} + \left(\frac{\dot{I}_b^c}{\dot{I}_S^c} + 1\right) Z_{bf} + \left(\frac{\dot{I}_b^c}{\dot{I}_S^c} + \frac{\dot{I}_{DG}^c}{\dot{I}_S^c} + 1\right) Z_f, \\ Z_{m(2)} &= Z_{Bf} + \left(\frac{\dot{I}_b^c}{\dot{I}_{DG}^c} + \frac{\dot{I}_S^c}{\dot{I}_{DG}^c} + 1\right) Z_f, \\ Z_{m(11)} &= Z_b + \left(\frac{\dot{I}_S^c}{\dot{I}_b^c} + 1\right) Z_{bf} + \left(\frac{\dot{I}_S^c}{\dot{I}_b^c} + \frac{\dot{I}_{DG}^c}{\dot{I}_b^c} + 1\right) Z_f, \\ \dot{I}_b^c &= \dot{I}_b + 3k_0 \dot{I}_b^0, \end{aligned} \tag{15}$$

where $\dot{I}_b^0$ is the zero-sequence fault current of the infeed branch.

The values of Z_{bf} and Z_f can be calculated through

$$\begin{aligned} Z_{bf}^c &= \frac{M \cdot P - K \cdot N}{J \cdot P - K \cdot L}, \\ Z_f^c &= \frac{J \cdot N - M \cdot L}{J \cdot P - K \cdot L}, \end{aligned} \tag{16}$$

where

$$\begin{aligned} M &= Z_{m(11)} - Z_b, \\ N &= Z_{m(1)} + Z_{m(2)} - Z_{AB}, \\ J &= \frac{\dot{I}_S^c}{\dot{I}_b^c} + 1, \\ K &= \frac{\dot{I}_S^c}{\dot{I}_b^c} + \frac{\dot{I}_{DG}^c}{\dot{I}_b^c} + 1, \\ L &= \frac{\dot{I}_b^c}{\dot{I}_S^c}, \\ P &= \frac{\dot{I}_b^c}{\dot{I}_S^c} + \frac{\dot{I}_{DG}^c}{\dot{I}_S^c} + \frac{\dot{I}_b^c}{\dot{I}_{DG}^c} + \frac{\dot{I}_S^c}{\dot{I}_{DG}^c} + 2. \end{aligned} \tag{17}$$

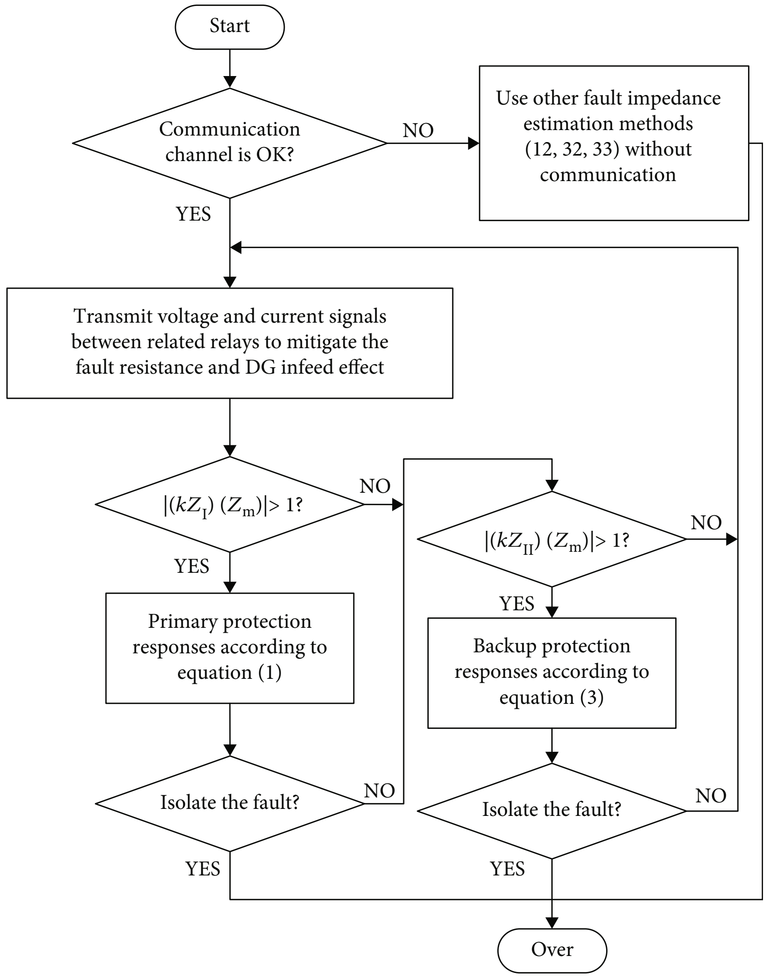

Figure 7: The schematic diagram of the ITD protection.

The measured impedance can be substituted by the calculated impedance shown in

$$\begin{aligned} Z^{c}_{m(1)} &= Z_{m(1)} - \left(\frac{\dot{I}^{c}_{b}}{\dot{I}^{c}_{S}} + \frac{\dot{I}^{c}_{DG}}{\dot{I}^{c}_{S}} + 1\right) Z^{c}_{f} - \left(\frac{\dot{I}^{c}_{b}}{\dot{I}^{c}_{S}}\right) Z^{c}_{bf}, \\ Z^{c}_{m(2)} &= Z_{m(2)} - \left(\frac{\dot{I}^{c}_{b}}{\dot{I}^{c}_{DG}} + \frac{\dot{I}^{c}_{S}}{\dot{I}^{c}_{DG}} + 1\right) Z^{c}_{f}, \\ Z^{c}_{m(11)} &= Z_{m(11)} - \left(\frac{\dot{I}^{c}_{S}}{\dot{I}^{c}_{b}} + \frac{\dot{I}^{c}_{DG}}{\dot{I}^{c}_{b}} + 1\right) Z^{c}_{f} - \left(\frac{\dot{I}^{c}_{S}}{\dot{I}^{c}_{b}}\right) Z^{c}_{bf}. \end{aligned} \tag{18}$$

It can be seen that the philosophy of the proposed method is utilising the remote-local current ratio to mitigate the errors in impedance measurement. The current ratio can be easily obtained by transmitting current signals between the related relays and using high-speed processors in digital relays.

In comparison with the ITA protection proposed in [22], the ITD protection has two advantages. First of all, the ITD protection uses single inverse-time characteristics, which is much simpler than the ITA protection. Secondly, the performance of the ITA protection can be easily affected by the fault resistance and DG infeed, which is considered and improved in the ITD protection.

2.4.3. Phase-to-Phase Fault. Likewise, the effect of the fault impedance and infeed on the measured impedance during a phase-to-phase fault can be mitigated by using the similar method mentioned above.

The proposed ITD protection can detect different types of faults with less operating time to improve the reliability of the network. The communication-assisted method can mitigate the fault impedance and the DG infeed effect by utilising the remote-local current ratio. The new ITD protection can solve the problems aforementioned at the ending of Section 1, and it is effective in both grid-connected and islanded modes. A protection scheme involving the proposed ITD protection is presented in the next section.

3. The Proposed Protection Scheme

The proposed ITD protection can be used for medium-voltage AC microgrids either in grid-connected or islanded mode. A protection scheme involving new protection

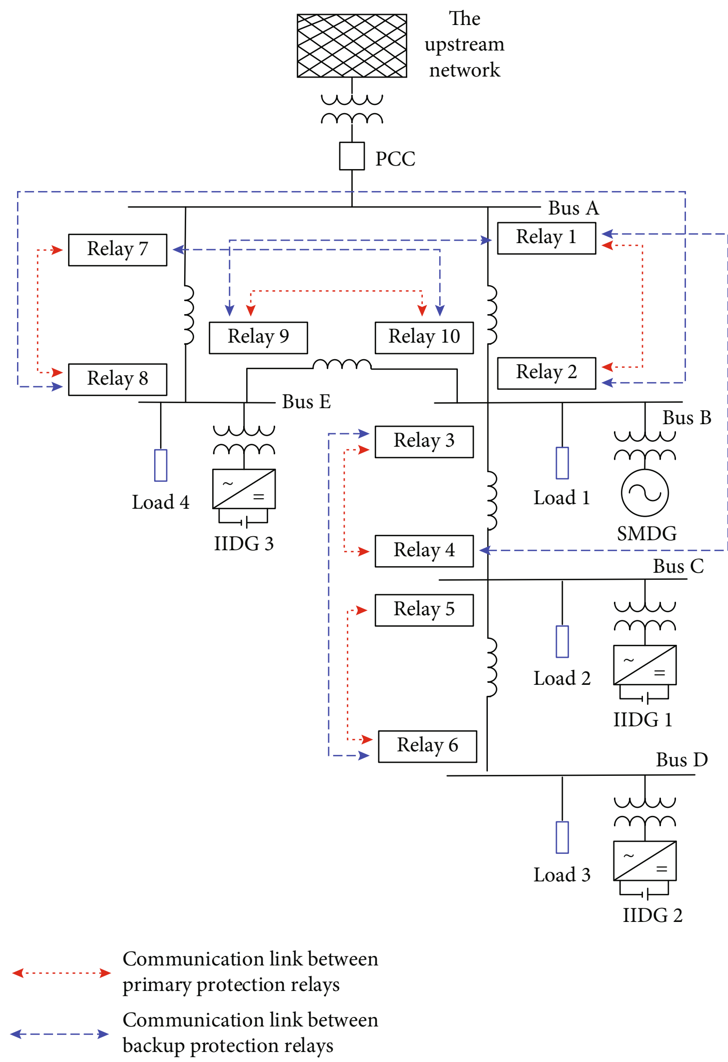

Figure 8: A sample AC microgrid interconnected with IIDGs.

methods has been established, and the schematic diagram is presented in Figure 7.

The communication channel is checked firstly, and voltage and current signals are transmitted between the related relays. Then, the remote-local current ratio is calculated by the digital relay to mitigate the fault impedance and DG infeed effect on the measured impedance. When the calculated impedance meets the primary protection requirement shown in (1), the fault would be detected and isolated with a less dependent time. The backup protection responds in the case when the primary protection fails to isolate the fault and the backup protection requirement is met. It is noted that the proposed method needs a robust communication system to transmit signals between the related relays. The communication channel time is discussed and compared with the relay operating time as the following. For the lengths of feeders that are normally short in microgrids, pilot wires, optical fibres, or Ethernet can be used to transmit signals. When the distance is less than 5 kilometers, the signal transmission takes less than 10 milliseconds [37], which is sufficient for ITD protection. On the other hand, the time-synchronised measurements are unnecessary for the proposed ITD protection, which means the proposed method is much more economical and convenient than the differential protection.

If a failure occurs in the communication system, the protection scheme transforms into other methods estimating the fault impedance without communication. Xu et al. presented the angle of the negative-sequence current distribution factor varying little during the fault and proposed an estimation algorithm to calculate the fault impedance both in phase-to-ground faults and phase-to-phase faults [38, 39]. These estimation methods can be used to calculate the fault impedance in the case when the communication system fails to respond.

4. Case Study

In order to investigate the effectiveness of the proposed method, a medium-voltage AC microgrid shown in Figure 8 was simulated in MATLAB Simulink.

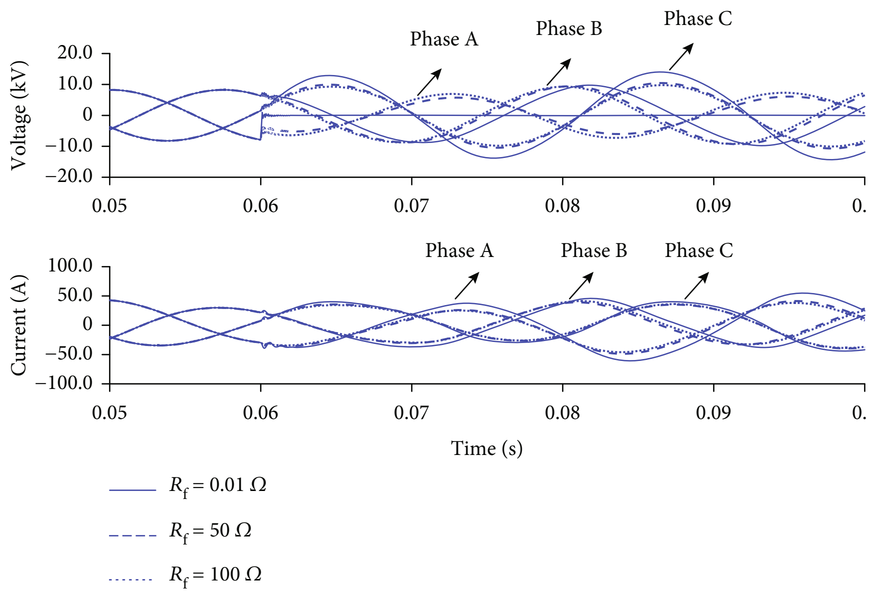

Figure 9: Voltages and currents seen by relay 1 during a single line-to-ground fault at 87.5% of the feeder AB.

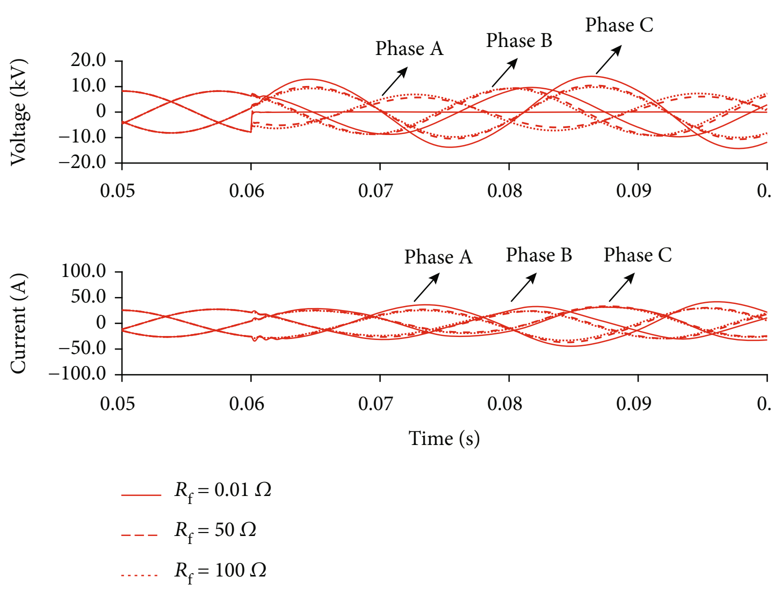

Figure 10: Voltages and currents seen by relay 2 during a single line-to-ground fault at 87.5% of the feeder AB.

The voltage level of the microgrid is 11 kV rms, and four DGs are interconnected with the network via coupling transformers. The output power of IIDG 1, IIDG 2, IIDG3, and SMDG are 0.50, 0.50, 0.40, and 0.80 MW, respectively. IIDGs are selected as photovoltaic generators. Feeders AB, BC, CD, AE, and BE are all same type overhead lines with a length of 3.0, 1.5, 2.0, 2.0, and 3.0 km, respectively. The resistance and reactance per unit length of the overhead line are 0.17 Ω/km and 0.38 Ω/km, respectively. The load connected at each bus is 0.4 MW to 0.8 MW with a power factor of 0.85 lagging. Relays represented as relay 1 to relay 10 are implemented at each side of the feeders, which involve the proposed ITD protection. The locations of the relays are shown in Figure 8 as well as the communication link between the related relays.

4.1. Fault Isolation in Islanded Mode. The microgrid can operate in islanded and grid-connected modes, depending on the statue of the common coupling point (PCC). When PCC is open, the microgrid is under the islanded mode. SMDG is under the V-f control strategy, while IIDGs are under the PQ control strategies.

When a single line-to-ground fault occurs at 87.5% of the feeder AB length, the voltages and currents seen by relay 1 and relay 2 are shown in Figures 9 and 10, respectively. It can be seen that the amplitudes of the fault currents are

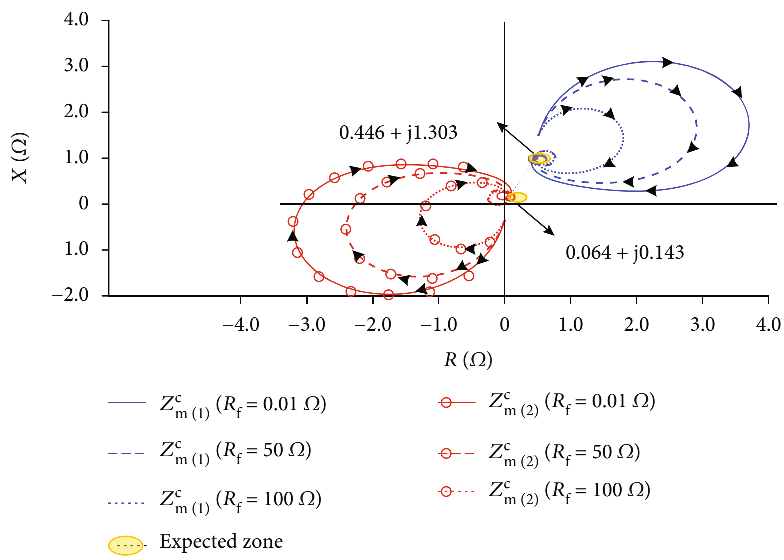

Figure 11: The calculated impedance of relay 1 and relay 2.

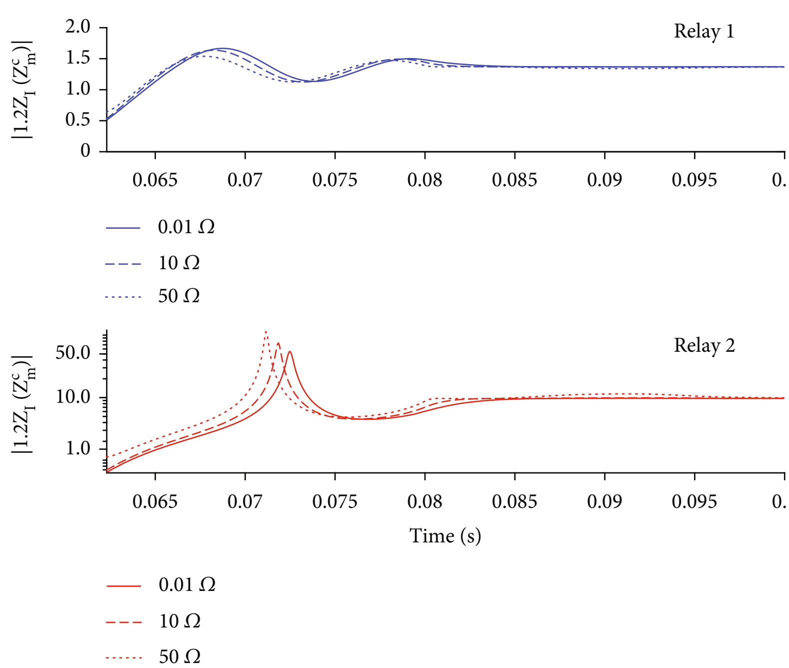

Figure 12: The simulation results of $|1.2ZI/Zm|$ of relay 1 and relay 2 during a SLG fault at 87.5% of the feeder AB.

lower than 50 A, which is the result that the fault currents are provided by DGs and limited by the DG capacity and control strategy.

The fundamental components of the voltage and current are extracted by using the fast Fourier transform (FFT), which are used to obtain the measured impedance. Due to the fault resistance and DG connection, the measured impedance values are inaccurate. To reduce the errors, the mitigating method proposed in this paper is implemented, and the calculated impedance of relay 1 and relay 2 is presented in Figure 11. It can be seen that the impedance values move into the expected zones where the values are $0.446 + j1.303\,\Omega$ and $0.064 + j0.143\,\Omega$, respectively.

The impedance values are utilised in ITA protection. The simulations of the impedance values of relay 1 and relay 2 are presented in Figure 12. The values of $1.2Z_I/Z_m$ stabilise at 1.398 and 9.638, respectively, after one cycle, and the calculation results are 1.371 and 9.600, respectively, which verifies the correctness of the simulation.

To verify the effectiveness of the proposed method, the phase-to-ground and phase-to-phase faults are both studied. The fault location is selected at 87.5% of the feeder AB length, and the fault resistance is considered. The ITD primary protection is implemented in relay 1 and relay 2, while the backup protection is in relay 1, relay 2, relay 4, relay 8, and relay 9. The simulation results of the relay operating

Table 1: Relay operating time (s) during a fault occurring at 87.5% of the feeder AB in the islanded mode.

ITA protection relay		Simulation results L-G Fault resistance (Ω) 0.01	50	100	LL Fault resistance (Ω) 0.01	5	10	LL-G Fault resistance (Ω) 0.01	50	100	LLL Fault resistance (Ω) 0.01	5	10	Calculation results
Primary protection	1	0.151	0.149	0.146	0.151	0.152	0.152	0.141	0.151	0.151	0.149	0.149	0.151	0.150
	2	0.001	0.001	0.001	0.002	0.002	0.002	0.002	0.001	0.001	0.003	0.001	0.001	0.001
Backup protection	1	0.559	0.572	0.581	0.560	0.559	0.562	0.570	0.561	0.563	0.589	0.563	0.565	0.581
	2	0.557	0.558	0.561	0.557	0.557	0.557	0.556	0.557	0.557	0.559	0.557	0.557	0.557
	4	0.632	0.614	0.608	0.634	0.631	0.626	0.625	0.626	0.624	0.600	0.623	0.621	0.607
	8	0.780	0.712	0.679	0.779	0.761	0.749	0.803	0.750	0.745	0.723	0.754	0.742	0.775
	9	0.761	0.654	0.619	0.713	0.730	0.741	0.722	0.741	0.728	0.603	0.707	0.717	0.776

Table 2: Relay operating time (s) during a fault occurring at 12.5% of the feeder AB in the grid-connected mode.

ITA protection relay		Simulation results L-G Fault resistance (Ω) 0.01	50	100	LL Fault resistance (Ω) 0.01	5	10	LL-G Fault resistance (Ω) 0.01	50	100	LLL Fault resistance (Ω) 0.01	5	10	Calculation results
Primary protection	1	0.001	0.001	0.001	0.001	0.001	0.001	0.001	0.001	0.001	0.001	0.001	0.001	0.001
	2	0.150	0.153	0.156	0.151	0.151	0.152	0.149	0.151	0.151	0.149	0.149	0.151	0.150
Backup protection	1	0.542	0.544	0.547	0.541	0.542	0.542	0.541	0.541	0.541	0.541	0.542	0.543	0.541
	2	0.572	0.571	0.571	0.573	0.572	0.574	0.572	0.571	0.576	0.572	0.572	0.574	0.573
	4	0.796	0.711	0.676	0.800	0.772	0.752	0.799	0.800	0.800	0.806	0.773	0.753	0.774
	8	—	—	—	—	—	—	—	—	—	—	—	—	—
	9	0.822	0.736	0.698	0.782	0.762	0.746	0.812	0.783	0.782	0.777	0.766	0.750	0.778

time are tabulated in Table 1 as well as the calculation results.

It can be seen from Table 1 that the ITD primary protection can detect the fault within 0.15 seconds to meet the FRT requirements. The backup protection can be coordinated, and the CTIs are larger than 0.3 seconds. With the presence of the fault resistance and DG, the effect on the measured impedance can be mitigated by using the proposed method. The maximum errors between the simulation and calculation results are 0.002 seconds in primary protection and 0.069 seconds in backup protection. The effectiveness of the proposed method is verified under the islanded mode.

4.2. Fault Isolation in Grid-Connected Mode. When PCC is close, the microgrid is in the grid-connected mode and all DGs are under the PQ control strategy.

The fault location is selected at 12.5% of the feeder AB length, and different fault types are studied. The primary protection is implemented in relay 1 and relay 2, while the backup protection is in relay 1, relay 2, relay 4, and relay 9. The operation times of relays involving ITA protection are presented in Table 2. It can be seen that the performance of the ITD protection can also meet the FRT requirements and detect HIFs. The ITD protection can detect faults whatever the operation mode is, which is effective for AC microgrid.

4.3. Comparison with the Distance Protection. The ITD protection has been tested and compared with the method proposed in [30]. The FRT requirements were considered, while the HIF detection was inefficient in [30]. When a SLG fault occurs at 50% of the feeder AB, the measured impedances of relay 1 under different scenarios are simulated and presented in Figure 13. The Z_{set}^{I} of zone 1 is $0.204 + j0.456\,\Omega$ according to [30]. It can be seen that the measured impedance value is $0.146 + j0.275\,\Omega$ and the value moves into the zone 1 reach when the fault resistance is $0.01\,\Omega$. However, when the fault resistance increases to $50\,\Omega$ and $100\,\Omega$, respectively, the measured impedance values move a lot beyond the zone 1 reach and it is inefficient in the HIF detection.

Likewise, faults occurring in the feeder AB in the islanded mode were tested, and the results are compared in Table 3. The average relay operating time of ITD method is 0.054 s, and the average relay operating time of the method proposed in [30] is 0.191 s. The ITD protection performs much better than the method proposed in [30].

The ITD protection proposed in this paper is compared with some prior-art methods, and the comparisons are presented in Table 4 as well. The FRT requirements, the HIF detection, the fault types, and the communication are contained in the comparison. For instance, the FRT requirements are considered in the proposed ITD protection, while they are not mentioned in the methods proposed in [25–27, 29]. The HIF are studied in the ITD protection, but the HIF detection is inefficient in the methods proposed in [26, 27, 30]. The ITD protection performs better than the prior-art methods listed in Table 4.

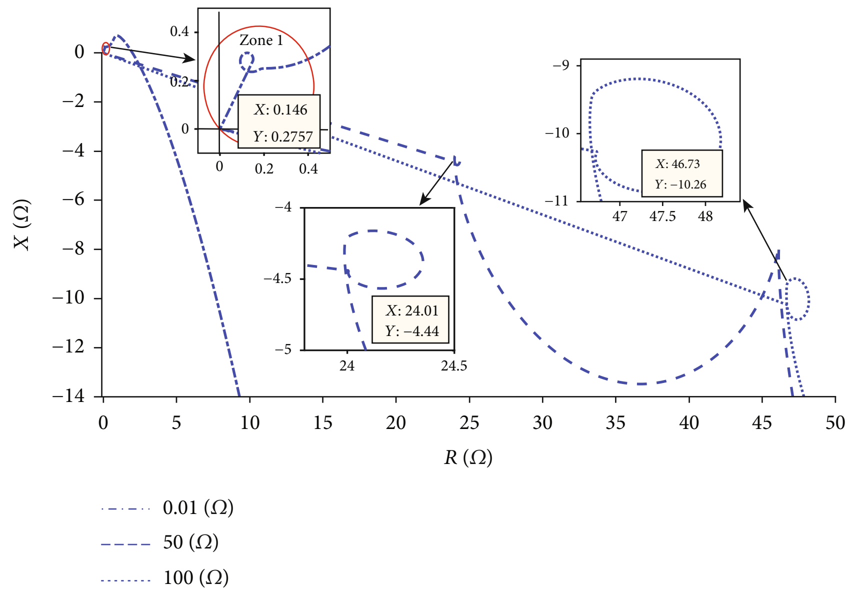

Figure 13: The measured impedance of relay 1 during a SLG fault at 50% of the feeder AB.

Table 3: Relay operating time (s) during a fault occurring in the feeder AB in the islanded mode.

Fault location	Fault resistance (Ω)	ITD method Relay 1	ITD method Relay 2	Method in [30] Relay 1	Method in [30] Relay 2
12.5%	0.01	0.001	0.151	0.001	0.380
	50	0.003	0.158	—	—
	100	0.006	0.143	—	—
20.0%	0.01	0.009	0.066	0.001	0.380
	50	0.006	0.082	—	—
	100	0.009	0.066	—	—
50.0%	0.01	0.028	0.028	0.001	0.380
	50	0.032	0.024	—	—
	100	0.038	0.020	—	—
80.0%	0.01	0.104	0.004	0.380	0.001
	50	0.110	0.003	—	—
	100	0.116	0.003	—	—
87.5%	0.01	0.151	0.001	0.380	0.001
	50	0.152	0.001	—	—
	100	0.157	0.001	—	—

Table 4: Comparison with some prior-art methods.

Description	Method in [25]	Method in [26]	Method in [27]	Method in [28]	Method in [29]	Method in [30]	ITD method
FRT considered	No	No	No	Yes	No	Yes	Yes
HIF studied	Excellent	Poor	Poor	Average	Average	Poor	Excellent
Fault types studied	Unbalanced faults	LLL-G faults	All types	All types	All types	All types	All types
Communication assisted	No	No	Yes	No	Yes	No	Yes

5. Conclusion

The conventional distance protection approaches are ineffective in detecting HIFs in microgrids and rarely consider the FRT requirements. To solve the two problems, a communication-assisted ITD protection has been proposed in this paper, based on the inverse-time characteristics and distance protection. The ITD primary protection can meet the FRT requirements, while the backup protection can be coordinated with a minimum time interval of 0.3 seconds. The communication-assisted method proposed in this paper can reduce the measured impedance error and improve the performance of the protection. The effectiveness of the ITD protection has been verified by time domain simulations. Since the feeders are short and the transmission time is sufficient for the proposed ITD protection, it can be used to detect faults in AC microgrids.

Data Availability

Data will be made available on request.

Conflicts of Interest

The authors declare that they have no conflicts of interest.

Acknowledgments

This work was supported by the National Science Foundation of China (Grant No. U20B2029); the National Key R&D Program Project of China (2023YFC2810902); the Special Scientific Research Foundation of the Education Department of Shaanxi Province, China (No. 23JK0386); the Scientific Research Fund Project of Shaanxi Railway Institute (No. KY2022-20); and the Education and Teaching Research Project of Shaanxi Railway Institute (No. 2021JG-22).

References

[1] A. Hooshyar and R. Iravani, "Microgrid protection," *Proceedings of the IEEE*, vol. 105, no. 7, pp. 1332–1353, 2017.

[2] S. K. Rangu, P. R. Lolla, K. R. Dhenuvakonda, and A. R. Singh, "Recent trends in power management strategies for optimal operation of distributed energy resources in microgrids: a comprehensive review," *International Journal of Energy Research*, vol. 44, no. 13, pp. 1332–9911, 2020.

[3] S. A. Gopalan, V. Sreeram, and H. H. Iu, "A review of coordination strategies and protection schemes for microgrids," *Renewable and Sustainable Energy Reviews*, vol. 32, pp. 222–228, 2014.

[4] H. D. Tafti, A. I. Maswood, G. Konstantinou et al., "Low-voltage ride-thorough capability of photovoltaic grid-connected neutral-point-clamped inverters with active/reactive power injection," *IET Renewable Power Generation*, vol. 11, no. 8, pp. 1182–1190, 2017.

[5] X. Liu, X. Zheng, Y. He, G. Zeng, and Y. Zhou, "Passive islanding detection method for grid-connected inverters based on closed-loop frequency control," *Journal of Electrical Engineering & Technology*, vol. 14, no. 6, pp. 2323–2332, 2019.

[6] S. Sarangi, B. K. Sahu, and P. K. Rout, "Review of distributed generator integrated AC microgrid protection: issues, strategies, and future trends," *International Journal of Energy Research*, vol. 45, no. 10, pp. 14117–14144, 2021.

[7] P. T. Manditereza and R. Bansal, "Renewable distributed generation: the hidden challenges–a review from the protection perspective," *Renewable and Sustainable Energy Reviews*, vol. 58, pp. 1457–1465, 2016.

[8] P. H. Shaikh, A. Shaikh, Z. A. Memon, A. A. Lashari, and Z. H. Leghari, "Microgrids: a review on optimal hybrid technologies, configurations, and applications," *International Journal of Energy Research*, vol. 45, no. 9, pp. 12564–12597, 2021.

[9] U. Orji, C. Schantz, S. B. Leeb et al., "Adaptive Zonal Protection for Ring Microgrids," *IEEE Transactions on Smart Grid*, vol. 8, no. 4, pp. 1843–1851, 2017.

[10] A. Oudalov and A. Fidigatti, "Adaptive network protection in microgrids," *International Journal of Distributed Energy Resources*, vol. 5, no. 3, pp. 201–226, 2009.

[11] H. M. Sharaf, H. H. Zeineldin, and E. El-Saadany, "Protection Coordination for Microgrids With Grid-Connected and Islanded Capabilities Using Communication Assisted Dual Setting Directional Overcurrent Relays," *IEEE Transactions on Smart Grid*, vol. 9, no. 1, pp. 143–151, 2018.

[12] M. Singh and P. Basak, "Adaptive protection methodology in microgrid for fault location and nature detection usingq0 components of fault current," *IET Generation, Transmission & Distribution*, vol. 13, no. 6, pp. 760–769, 2019.

[13] T. S. Aghdam, H. K. Karegar, and H. H. Zeineldin, "Variable tripping time differential protection for microgrids considering DG stability," *IEEE Transactions on Smart Grid*, vol. 10, no. 3, pp. 2407–2415, 2019.

[14] A. Soleimanisardoo, H. K. Karegar, and H. H. Zeineldin, "Differential frequency protection scheme based on off-nominal frequency injections for inverter-based islanded microgrids," *IEEE Transactions on Smart Grid*, vol. 10, no. 2, pp. 2107–2114, 2019.

[15] Z. Chen, X. Pei, M. Yang, L. Peng, and P. Shi, "A novel protection scheme for inverter-interfaced microgrid (IIM) operated in islanded mode," *IEEE Transactions on Power Electronics*, vol. 33, no. 9, pp. 7684–7697, 2017.

[16] M. T. Faiz, D. Khan, M. M. Khan, A. Ali, and H. Tang, "Improved stability and damping characteristics of *LCL*-filter based distributed generation system," *Journal of Electrical Engineering & Technology*, vol. 16, no. 3, pp. 1619–1635, 2021.

[17] D. K. Ibrahim, E. E. D. A. El Zahab, and S. A. E. A. Mostafa, "New coordination approach to minimize the number of re-adjusted relays when adding DGs in interconnected power systems with a minimum value of fault current limiter," *International Journal of Electrical Power & Energy Systems*, vol. 85, pp. 32–41, 2017.

[18] H. Al-Nasseri, M. A. Redfern, and F. Li, "A voltage based protection for micro-grids containing power electronic converters," in *2006 IEEE Power Engineering Society General Meeting*, p. 7, Montreal, QC, Canada, 2006.

[19] T. Loix, T. Wijnhoven, and G. Deconinck, "Protection of microgrids with a high penetration of inverter-coupled energy sources," in *2009 CIGRE/IEEE PES Joint Symposium Integration of Wide-Scale Renewable Resources Into the Power Delivery System*, pp. 1–6, Calgary, AB, Canada, 2009.

[20] C. R. Reddy and K. H. Reddy, "A new passive islanding detection technique for integrated distributed generation system

using rate of change of regulator voltage over reactive power at balanced islanding," *Journal of Electrical Engineering & Technology*, vol. 14, no. 2, pp. 527–534, 2019.

[21] F. Zhang and L. Mu, "A Fault Detection Method of Microgrids With Grid-Connected Inverter Interfaced Distributed Generators Based on the PQ Control Strategy," *IEEE Transactions on Smart Grid*, vol. 10, no. 5, pp. 4816–4826, 2019.

[22] M. Dewadasa, A. Ghosh, G. Ledwich, and M. Wishart, "Fault isolation in distributed generation connected distribution networks," *IET Generation, Transmission & Distribution*, vol. 5, no. 10, pp. 1053–1061, 2011.

[23] A. Sinclair, D. Finney, D. Martin, and P. Sharma, "Distance Protection in Distribution Systems: How It Assists With Integrating Distributed Resources," *IEEE Transactions on Industry Applications*, vol. 50, no. 3, pp. 2186–2196, 2014.

[24] J. H. Lee, M. S. Park, H. S. Ahn et al., "Method for protection of single-line-ground fault of distribution system with DG using distance relay and directional relay," *Journal of Electrical Engineering & Technology*, vol. 15, no. 4, pp. 1607–1616, 2020.

[25] Y. Liang, W. Li, and W. Zha, "Adaptive Mho Characteristic-Based Distance Protection for Lines Emanating From Photovoltaic Power Plants Under Unbalanced Faults," *IEEE Systems Journal*, vol. 15, no. 3, pp. 3506–3516, 2021.

[26] F. M. AlAlamat, E. A. Feilat, and M. A. Haj-ahmed, "New Distance Protection Scheme for PV Microgrids," in *2020 6th IEEE International Energy Conference (ENERGYCon)*, pp. 668–673, Gammarth, Tunisia, 2020.

[27] S. Biswas and V. Centeno, "A communication based infeed correction method for distance protection in distribution systems," in *2017 North American Power Symposium (NAPS)*, pp. 1–5, Morgantown, WV, USA, 2017.

[28] K. Jia, J. Chen, Z. Xuan, C. Wang, and T. Bi, "Active protection for photovoltaic DC-boosting integration system during FRT," *IET Generation, Transmission & Distribution*, vol. 13, no. 18, pp. 4081–4088, 2019.

[29] A. Hooshyar, M. A. Azzouz, and E. F. El-Saadany, "Distance Protection of Lines Emanating From Full-Scale Converter-Interfaced Renewable Energy Power Plants—Part II: Solution Description and Evaluation," *IEEE Transactions on Power Delivery*, vol. 30, no. 4, pp. 1781–1791, 2015.

[30] H. Lin, C. Liu, J. M. Guerrero, and J. C. Vásquez, "Distance protection for microgrids in distribution system," in *IECON 2015 - 41st Annual Conference of the IEEE Industrial Electronics Society*, pp. 000731–000736, Yokohama, Japan, 2015.

[31] E. Troester, "New German grid codes for connecting PV systems to the medium voltage power grid," in *2nd International workshop on concentrating photovoltaic power plants: optical design, production, grid connection*, pp. 1–4, Darmstadt, Germany, 2009.

[32] IEEE, *IEEE standard for inverse-time characteristics equations for overcurrent relays. IEEE Std C37112-2018 (Revision of IEEE Std C37112-1996)*, IEEE Power and Energy Society, 2019.

[33] L. Ji, Z. Cao, Q. Hong et al., "An improved inverse-time overcurrent protection method for a microgrid with optimized acceleration and coordination," *Energies*, vol. 13, no. 21, p. 5726, 2020.

[34] W. A. Elmore, *Protective relaying: theory and applications*, vol. 1, CRC press, 2003.

[35] H. Muda and P. Jena, "Superimposed Adaptive Sequence Current Based Microgrid Protection: A New Technique," *IEEE Transactions on Power Delivery*, vol. 32, no. 2, pp. 757–767, 2017.

[36] H. S. Hosseini, A. Koochaki, and S. H. Hosseinian, "A novel scheme for current only directional overcurrent protection based on post-fault current phasor estimation," *Journal of Electrical Engineering & Technology*, vol. 14, no. 4, pp. 1517–1527, 2019.

[37] E. Sortomme, S. S. Venkata, and J. Mitra, "Microgrid Protection Using Communication-Assisted Digital Relays," *IEEE Transactions on Power Delivery*, vol. 25, no. 4, pp. 2789–2796, 2010.

[38] Z. Y. Xu, S. J. Jiang, Q. X. Yang, and T. S. Bi, "Ground distance relaying algorithm for high resistance fault," *IET generation, Transmission & Distribution*, vol. 4, no. 1, pp. 27–35, 2010.

[39] Z. Y. Xu, S. J. Jiang, and L. Ran, "Phase distance relaying algorithm for unbalanced inter-phase faults," *IET Generation, Transmission & Distribution*, vol. 4, no. 12, pp. 1326–1333, 2010.